GNSS Receive Antennas on Satellites for Precision Orbit Determination

Jan Zackrisson, Mikael Öhgren
RUAG Space AB
SE-405 15 Goteborg, Sweden ; +46 31 7354004
jan.zackrisson@ruag.com

ABSTRACT

This paper presents GNSS (Global Navigation Satellite System) antennas developed for different earth observation missions. Such missions often require Precise Orbit Determination (POD). The largest error contribution to POD measurements is usually local multipath, i.e. signals reflected in the satellite structure. Antenna radiation in the back direction must hence be suppressed, while at the same time keep a good coverage at low elevation angles. This is normally achieved by using a standard antenna element placed in a larger choke ring structure. The disadvantage with this arrangement is that the antenna becomes large and relatively heavy. The objective has hence been to develop small and lightweight antennas with low back radiation in combination with good coverage. We have worked with both low profile Patch Excited Cup (PEC), as well as helix antennas. Two of the described antennas are PEC antennas. One smaller, suitable on satellites without large flat mounting areas, and one design where the low elevation gain was traded against the back radiation and a good compromise was achieved using only two narrow choke rings to facilitate mounting on larger flat surfaces. A high-performance conical quadrifilar helix antenna has earlier been developed for applications where a taller antenna can be accommodated.

INTRODUCTION

RUAG Space has during the last thirty years developed a large family of wide coverage antennas.[5, 6, 7]

The antennas are and have been used for a number of satellite applications including telemetry and command, beacon, data downlinks, GPS reception and also for launch vehicles. We have used the PEC antenna technology for several of the applications.[1, 3]

In this paper we present several GNSS (Global Navigation Satellite System) antennas developed for different missions. [8, 9, 10, 11]

The largest error contribution for the position measurements is usually local multipath, i.e. signals reflected in the satellite structure. The design work has then concentrated on the antenna radiation in the back direction, which must be suppressed, and the possibility to at the same time keep a good coverage at low elevation angles. Normally these requirements are achieved by using a standard antenna element placed in a larger choke ring structure. The disadvantage with this antenna type is that the antenna becomes large, with a diameter of more than 300 mm, and thus relatively heavy. Our objective has hence been to develop small and lightweight antennas with low back radiation in combination with good coverage. Both low profile PEC antennas, as well as helix antennas have been used for this. Below examples of these antennas are presented.

PATCH EXCITED CUP ANTENNA DESIGN

Two PEC antennas are described in this section. First the PEC antenna without a choke-ring will be dealt with. It is similar to an S-band antenna delivered to the GOCE project.[4] The GOCE antenna consists of two patches, placed in a circular cup. The bottom patch is capacitively fed by two probes. For the new L-band antenna we needed a very stable antenna covering the GNSS frequency bands. This has been obtained by using a four-point feed with capacitive coupling of the bottom patch, and an isolated feed network.

The PEC antenna consists then of two stacked patches placed in a short cylindrical cup. The upper patch in the antenna element is electromagnetically coupled to the lower patch and the lower patch is fed in phase quadrature at four points from a stripline feed network. The feed network is isolated and has four feed points to the lower patch with 0, 90, 180, and 270 degrees phase for generation of circular polarization.

The radiation and matching characteristics of the PEC antenna can be optimised almost separately from each other. The radiation characteristics are mainly affected by the aperture diameter, cup height and top patch dimensions. The matching is achieved by varying the bottom patch dimensions and feed probe positions. There is of course some influence across this “design separation”, but that is readily handled.

The design starts by optimising the radiation pattern. Although the final performance requirements are normally set for the radiator located on a satellite structure, it is best to work with the PEC antenna standing alone. In order to do this we add the soft requirement that the back radiation should be minimised while keeping sufficient gain at 80°. This includes both co- and cross-polarisation. It was verified in a later step that the antenna mounted on the satellite structure would provide satisfactory radiation patterns.

If there is good match between the feed network and the PEC antenna radiator, they can be designed independently. For the radiator, it is then the active reflection coefficient that must be considered.

Using Ansoft HFSS software, the PEC antenna geometry was modelled with special attention to the feed probes. The electromagnetic model is shown in figure 1. The dimensions were varied systematically, in order to find both good radiation pattern performance and a good active match. The final active match result is shown in figure 2.

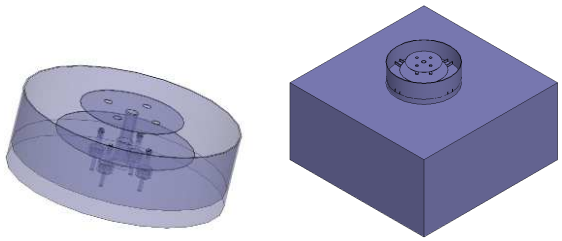

Figure 1: Electromagnetic model of the PEC antenna without choke ring (standalone and on a ground-plane)

The feed network consists of one input port and four outputs. The outputs should have equal amplitude and quadrature phase. In order to achieve this, broadband components are needed. The stripline network is built up with 3 dB / 90° hybrid couplers, a Schiffman phase shifter and ferrite loads.

The hybrid split the power in two equal parts, providing 0° and 90° outputs. It is used at the input of the network.

The Schiffman phase shifter achieves a 180° phase shift that matches the phase slope of a 270° line. This provides an additional broadband 90° phase difference between the 0° and 90° outputs of the hybrid, thus providing 0° and 180° signals of equal amplitude.

Finally, two more hybrids are used to end up with the four required output signals.

The ferrite loads are placed at the "silent" ports of the hybrids in order to absorb leakage, unwanted reflections and antenna cross polarised signals.

Behind the ferrite absorbers, grounding foils are used to achieve a DC ground path to avoid any free floating metal parts inside the antenna.

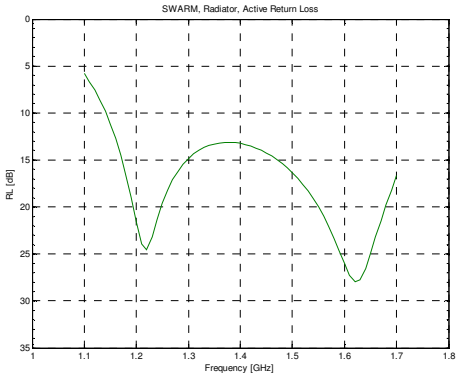

Figure 2: PEC antenna without choke ring, radiator active return loss

Figure 3 show three flight models of the antenna.

The final dimensions are a diameter of 160 mm and a height of 55 mm. The final mass is less than 320 g. It has a SMA connector RF interface.

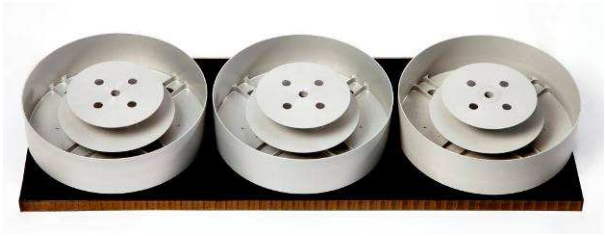

Figure 3: Three flight models of the PEC antenna without choke ring

Typical measured radiation performance for the antenna is shown below. It is gain min/average/max envelopes for six antennas over the hemisphere for co- and cross-polar radiation (co in red, cross in blue).

The predicted performance, from the HFSS analysis, is also shown in the figures (in green).

A typical measured return loss curve for the antenna is also shown below in figure 7.

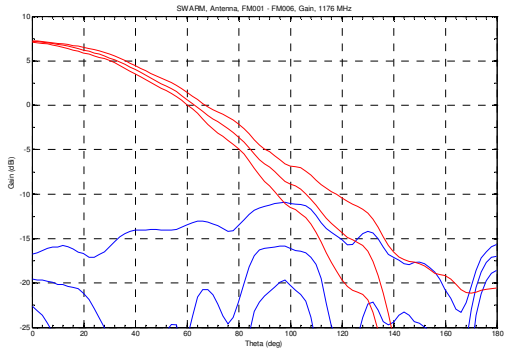

Figure 4: L5/E5a Frequency (1176.45 MHz), Radiation Pattern, PEC antenna without choke ring

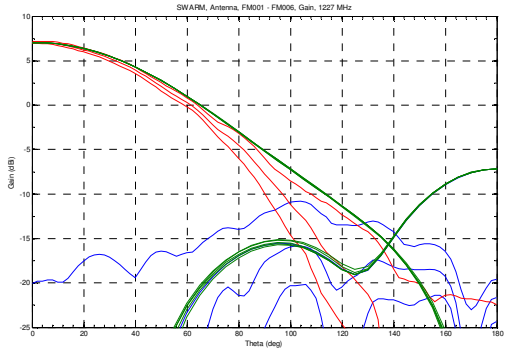

Figure 5: L2 Frequency (1227.6 MHz), Radiation Pattern, PEC antenna without choke ring

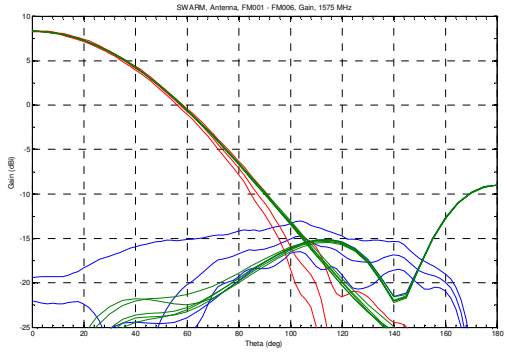

Figure 6: L1/E1 Frequency (1575.42 MHz), Radiation Pattern, PEC antenna without choke ring

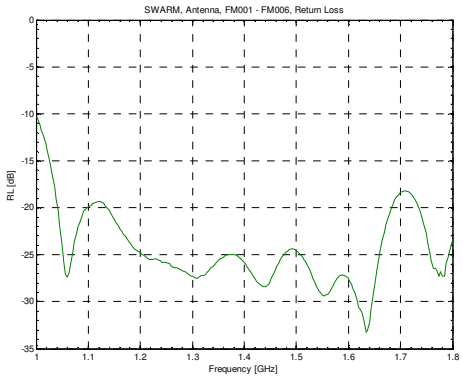

Figure 7: PEC antenna without choke ring, return loss

The benefit with the basic antenna without a choke-ring is the low profile, lightweight design and RF-performance. But the disadvantage is that this antenna has relatively large back radiation that could lead to high interference with the S/C. It was designed with strict volume restrictions. Since it was mounted on wedge-type spacecrafts without a flat ground-plane, the performance was good.

For applications where the antenna is mounted above a large flat ground-plane and thus demanding very low back radiation a new version of the PEC antenna was needed.

Therefore we have designed another PEC antenna, with two choke rings, which is less sensitive to the S/C structure.

The PEC antenna with two choke rings was designed in the same way as the basic antenna without a choke-ring. Using HFSS also for this antenna, the PEC geometry was modelled, and the HFSS model is shown in figure 8.

The active matching result is shown in figure 9.

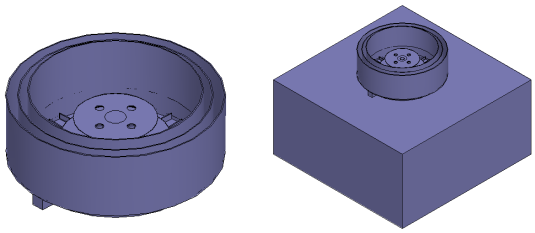

Figure 8: Electromagnetic model of the PEC antenna with two choke rings (standalone and on a ground-plane)

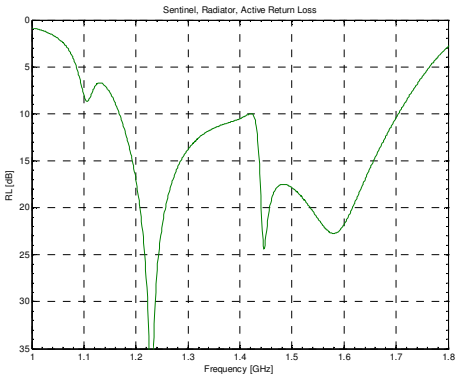

Figure 9: PEC antenna with two choke rings, radiator active return loss

Figure 10 show four flight models of the choke-ring antenna. The final dimensions are a diameter of 200 mm and a height of 75 mm. The final mass is less than 715 g. It has a SMA connector RF interface.

Figure 10: Four flight models of the PEC antenna with two choke rings

Typical measured radiation performance for the antenna is shown below. It is gain min/average/max envelopes for three antennas over the hemisphere for co- and cross-polar radiation (co in red, cross in blue). The predicted performance, from the HFSS analysis, is also shown in the figures (in green). A typical return loss curve for the antennas is also shown below in figure 14.

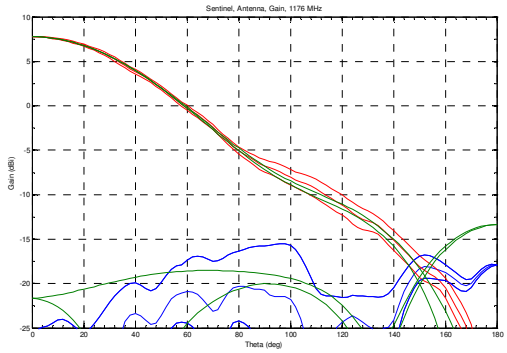

Figure 11: L5/E5a Frequency (1176.45 MHz), Radiation Pattern, PEC antenna with two choke rings

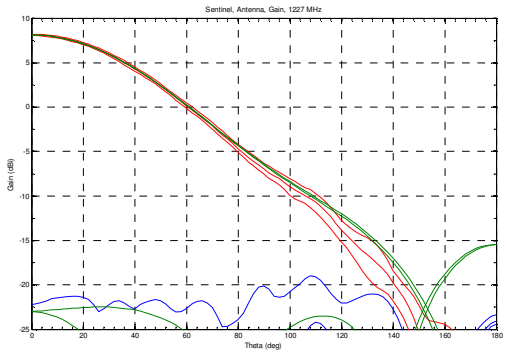

Figure 12: L2 Frequency (1227.6 MHz), Radiation Pattern, PEC antenna with two choke rings

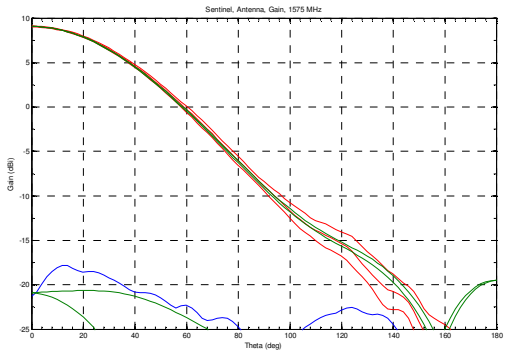

Figure 13: L1/E1 Frequency (1575.42 MHz), Radiation Pattern, PEC antenna with two choke rings

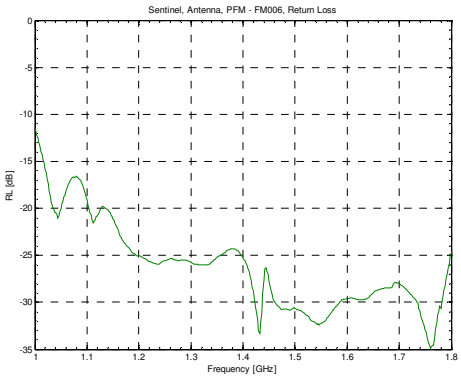

Figure 14: PEC antenna with two choke rings, return loss

THE SWARM SATELLITES

The ESA SWARM mission will provide a survey of the geomagnetic field, with the objective to improve our understanding of the Earth's interior and climate. The mission consists of three satellites, two following the same orbit, and one in a separate orbit. With this

constellation, it is possible to retrieve also the dynamic properties of the field.

Very accurate orbit determination is necessary, therefore a high precision dual frequency GPS receiver is accommodated. Accurate measurement of several GPS satellites is made, and this data is processed on ground to arrive at sub decimetre position accuracy. Since antenna local multi-path is normally the largest error contribution, very precise knowledge of the carrier and code phase radiation patterns for the antenna accommodated on the spacecraft, S/C, is needed for the ground processing. For redundancy reasons, two complete receive chains are used, each connected to one antenna.

The three satellites are stowed as a package during launch, limiting the available space for the antenna. The system uses both the L1 and L2 bands. Coverage out to 80° zenith angle is needed, while simultaneously the cross-polar and co-polar back radiation must be minimized. Considerable effort has been spent to find the best antenna location and to optimise the total performance by balancing antenna coverage against S/C interference and multipath errors. The S/C layout is shown in figure 15.

We used here, the low profile antenna without choke rings. It was primarily optimized for this mission based on the SWARM requirements.

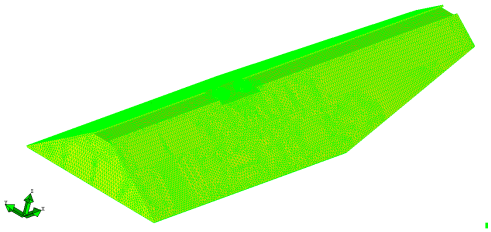

Figure 15: Electromagnetic model of the SWARM S/C including two antennas

THE SENTINEL SATELLITES

The Sentinel-1 to Sentinel -3 (S-1 to S-3) spacecrafts within the Global Monitoring for Environment and Security (GMES) programme are all equipped with GNSS POD receivers. The GNSS receiver is used to pinpoint measurements and is in the case of S-3 part of the radar altimeter measurement system, targeting cm accuracy.

POD processing is performed by adjusting the S/C orbit calculated from a force model, to several orbits of range measurement data. With a steady improvement of the modelling of the Earth gravitational field and other forces on the S/C, the accuracy of POD has steadily improved. One of the major POD error contributions is asymmetries and variations in the antenna phase pattern, partly caused by interference with the S/C. One way to control this is to use an antenna with a range of choke rings, which however becomes heavy and large and is often difficult to accommodate on a satellite.

The S1 to S3 S/C layouts can be seen in figure 16 to figure 18.

We used here our two choke ring GNSS antenna that covers all civil navigation frequency bands with excellent performance, low mass and small volume. It was primarily optimized for these mission based on the Sentinel requirements.

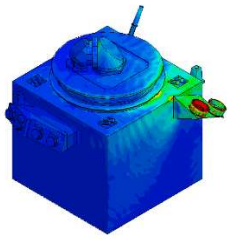

Figure 16: Electromagnetic model of the S-1 S/C including two antennas

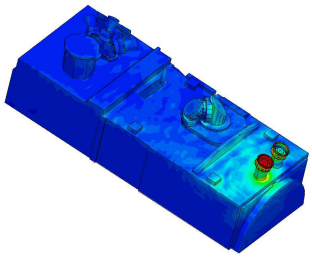

Figure 17: Electromagnetic model of the S-2 S/C including two antennas

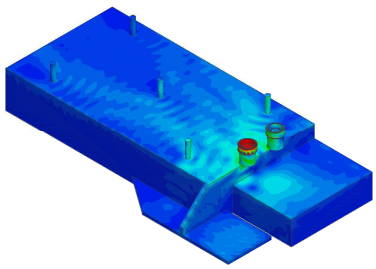

Figure 18: Electromagnetic model of the S-3 S/C including two antennas

ANTENNA PERFORMANCE ON SPACECRAFT

SWARM S/C, Antenna Performance

To finally characterize the antenna performance on satellite, it was measured on a mock-up.[2] Since the S/C interference is dominated by the structure close to the antennas, a limited mock-up can be used. The error due to the smaller mock-up has been evaluated by comparison between the Efield Multi-Level Fast Multipole Method (MLFMM) calculations with the complete S/C and with the different size mock-ups. Previously high frequency methods such as Physical Optics (PO) and Geometrical Theory of Diffraction (GTD) were the only way to simulate antenna performance of large objects. These methods have the drawback not to include coupling between the radiating object and the environment. However, the rapid development of EM simulation technique in combination with access to fast computers using parallel software gives new opportunities to simulate large objects.[8, 9]

The performance of the antenna including S/C interference was calculated with the Efield code using a model of the S/C. Small details compared to the wavelength were removed. The meshed S/C model is shown in figure 19 with the two antennas.

To measure a full size S/C structure with antennas in the antenna range was not seen as a realistic task. It was decided to use a smaller mock-up representing a part of the S/C for antenna characterization.

To select the proper size of the mock-up two different mock-up sizes were simulated, one larger with the overall length of 2.2 m and the same cross section as the S/C and one smaller mock-up with the length 1.5 m with cross section width reduced to 1.0 m. See figure 20. The simulation results were achieved using the same mesh parameters for all three models, the complete S/C, the larger mock-up and the smaller mock-up, in order to reduce numerical errors.

The radiation pattern interference with the S/C shows a global effect which is due to the ground-planes close to the antenna, and more rapid fluctuations due to interference from remote objects and edges. The rapid fluctuations are relatively small in amplitude and somewhat less confident. Therefore these fluctuations are filtered using Spherical Mode Expansion (SWE). Limiting the mode number included in the expansion, will result in a radiation pattern including only the global effect from the S/C interference. The rapid fluctuations are accepted as a characterisation error.

The smallest mock-up still gives the correct global impact on the antenna pattern and this is therefore selected for the mock-up tests on the antenna range.

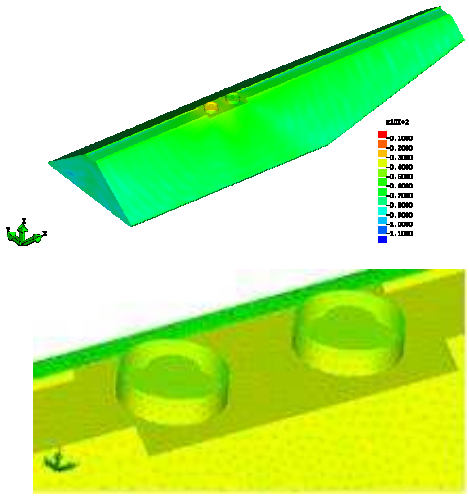

Figure 19: The meshed CAD model of the S/C including two antennas

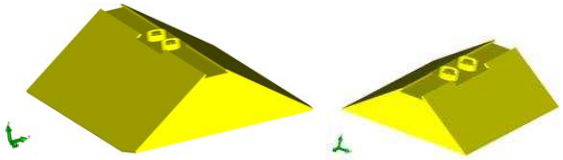

Figure 20: CAD models of the mock-ups, the larger 2 m one to the left and the smaller 1.5 m one to the right

The RF patterns for all flight models were tested on the selected size RF representative mock-up. Spherical near-field measurements were used in our 6 m indoor test range. The reduced size mock-up mounted in the range is shown in figure 21.

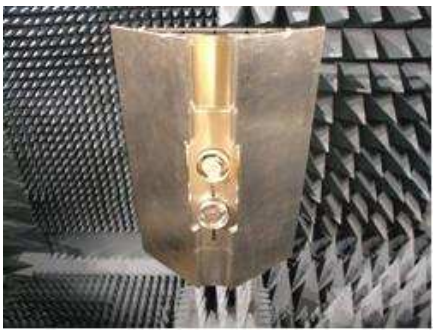

Figure 21: SWARM S/C mock-up on the test range

An example of radiation performance for the antenna on mock-up is shown below. It is gain min/max envelopes for all phi cuts for co- and cross-polar radiation.

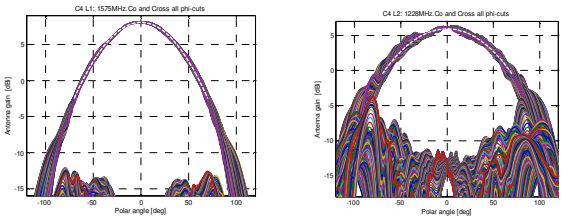

Figure 22: Co- and cross-polarization patterns, L1 to the left and L2 to the right

Sentinel S/C, Antenna Performance

To simulate and predict the radiation patterns for antennas installed on large objects such as spacecrafts is a challenging problem. Simulation tools based on Physical Optics (PO) and Geometrical Theory of Diffraction (GTD) have the disadvantage that they do not include the coupling between the radiating object and the environment and that the impact of the adjacent structure within the near field of the antenna is not included, as also discussed above.

In the Sentinel program we have instead used the electromagnetic tool Ansoft HFSS which is a FEM tool.[10, 11]

Thanks to the increasing computer speed and available memory size together with the rapid development of EM simulation techniques, very large structures can today be simulated.

We have modelled the whole spacecraft structure except for the solar panel in Ansoft HFSS. The output data of the software is the far field pattern which then was imported to the GRASP software from TICRA. In GRASP a model including the solar panel was built and the output of GRASP thus contains the far field information for the total S/C including solar panel.

Also for this programme it was concluded that to measure a full size S/C structure with antennas in the antenna range was not seen as a realistic task. It was thus decided to use a smaller mock-up representing a reduced part of the S/C for the antenna characterization.

The electromagnetic model for the Sentinel 3 S/C mock-up can be seen in figure 23.

In order to get a reasonable simulation model some simplification must be done. Small objects compared to wavelength have been removed.

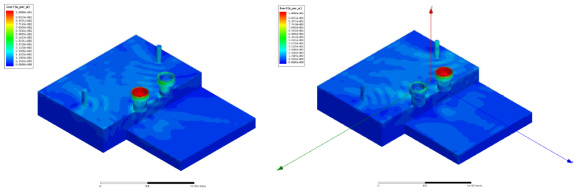

Figure 23: Electromagnetic model of the S-3 S/C mock-up

The mock-up mounted in the test range is shown in figure 24

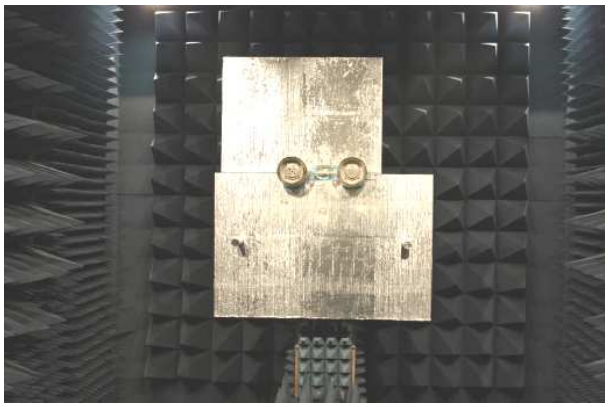

Figure 24: S-3 S/C mock-up on the test range

Radiation performance for the antenna on mock-up is shown below. It is a comparison between analysed and measured results.

Figure 25 show an example of the co-polar radiation pattern for measured and analysed data. Areas that can be used to verify the accuracy of the pattern are pointed out. The agreement between analysis and measurement is very good.

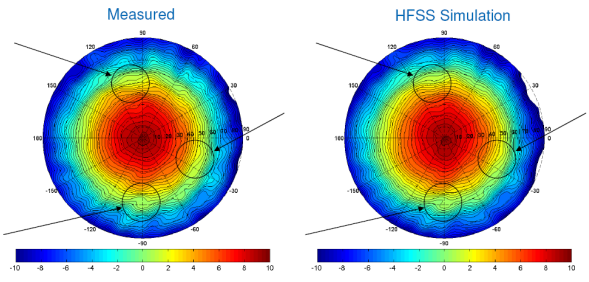

Figure 25: Measured and simulated co-polarization pattern of the S-3 S/C mock-up

Figure 26 show the cross-polar radiation pattern for measured and analysed data.

Also here a remarkable similarity can be seen between measured and analysed data.

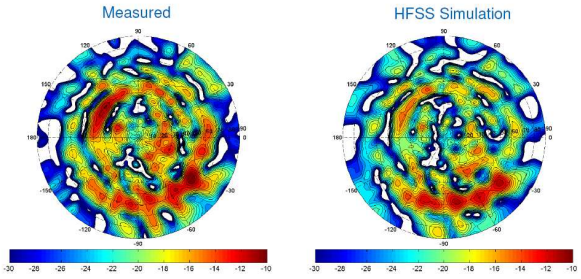

Figure 26: Measured and simulated cross-polarization pattern of the S-3 S/C mock-up

To demonstrate the accuracy the disturbance level, i.e. the difference between analysis and measurement are shown below in figure 27.

The disturbance level is around -20 dB in the worst areas and significantly lower for the larger part of the coverage area.

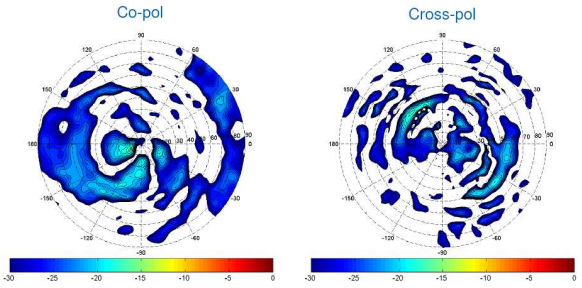

Figure 27: Disturbance level (accuracy), measured and simulated, co- and cross-polarization pattern of the S-3 S/C mock-up

HELIX ANTENNA DESIGN

The SWARM and Sentinel programmes used antennas with low height due to that the allowed height was restricted. A high-performance conical quadrifilar helix antenna was earlier developed for projects where a larger antenna could be accommodated.

The antenna can be used in the GPS L1 and L2 bands.

Quadrifilar helices give good circular polarisation over a large coverage, and by varying the helix dimensions, the coverage can be optimized to different requirements, like for a half sphere or isoflux coverage.

We use them extensively for TTC and data link applications. [5, 6, 7]

For this application, we needed a lightweight antenna, and thus used a printed cone one. These are usually fed from the bottom, leading to some back radiation. The application needed extremely low back radiation in order to, also here, minimize satellite disturbances. To fulfil this requirement we introduced a new patented feeding technique which reduced the back radiation by 5-10 dB.

The antenna can be equipped with an atomic oxygen protective cover, a germanium coated single layer insulation (SLI) foil, to allow the use of the antenna on low orbiting satellites.

The dimensions are a diameter of 90 mm and a height of 406 mm. The mass is less than 800 g. It has a TNC connector RF interface.

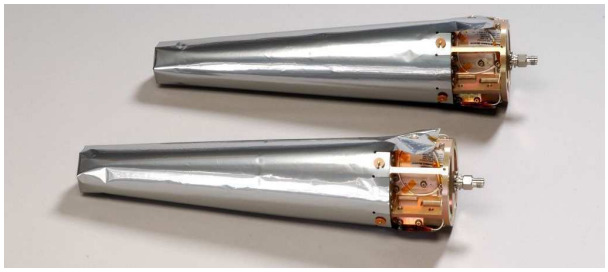

Figure 28: GPS helix antenna flight models with SLI cover

Typical measured radiation performance for the antenna is shown below. It is gain min/average/max envelopes for eighteen antennas over the hemisphere for co- and cross-polar radiation (co in red, cross in blue).

A typical return loss curve for the antennas is also shown below in figure 31.

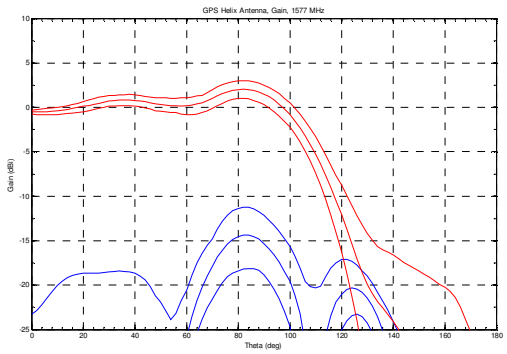

Figure 29: GPS helix antenna, L1 Frequency, radiation pattern (18 antennas min/max)

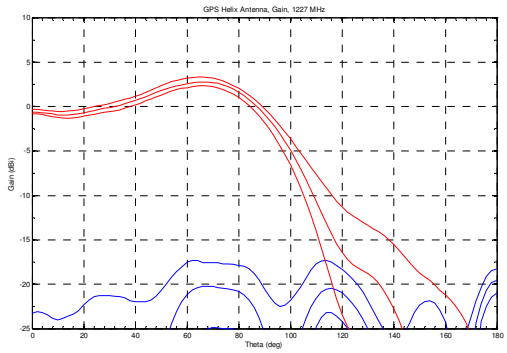

Figure 30: GPS helix antenna, L2 Frequency, radiation pattern (18 antennas min/max)

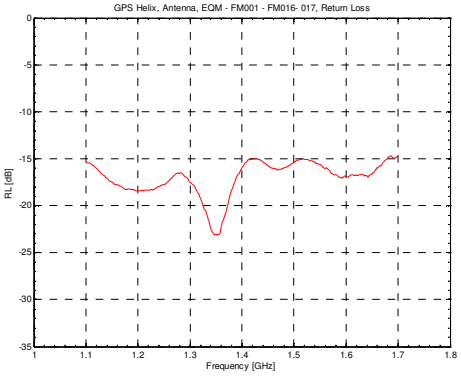

Figure 31: GPS helix antenna, return loss

ENVIRONMENTAL DESIGN ASPECTS

The normal thermal design for these types of antennas is passive. No MLI or other thermal hardware is used for thermal control. They are designed to perform over a wide temperature range, typically from - 150°C to + 150°C.

The antennas also need to survive a very harsh mechanical environment during launch, both random vibration and shock.

Atomic oxygen is also a factor to consider for LEO applications. This can be handled in a variety of ways, for example by using a germanium coated SLI protective cover as in the GPS helix antenna design. It can also be done using an atomic oxygen resistant surface treatment directly on the antenna as for the PEC antennas, where the outer surface is anodized.

REFERENCES

1. P. Svedjenäs, P. Hermansson, G. Jakobsson, F.S. Johansson, U. Jostell, B. Sundvall, "Patch Excited Cup Antenna for Spaceborne Mobile Communication Systems", Antenn 97, May 1997.

2. U. Larsson, T. Andersson, M. Öhgren, "Wide Coverage Satellite Antennas, GTD Analysis and Mock-Up Measurements", Antenn 00, May 2000.

3. P. Ingvarson, U. Jostell, P. Svedjenäs, "Patch Excited Cup Elements for Satellite Based Mobile Communication Antennas", IEEE International Conference on Phased Array Systems and Technology, May 2000.

4. P. Magnusson, G. Toso, "Low gain S-band antenna for the GOCE mission: a comparison between measurements and simulations with HFSS, CST Microwave Studio and FEKO", 26th ESA Antenna Technology Workshop on Satellite Antenna Modelling and Design Tools, ESA WPP-218, November 2003.

5. M. Öhgren, J. Zackrisson, P. Ingvarson, "Saab Ericsson Space History of Quadrifilar Helix Antennas", 28th ESA Antenna Workshop on Space Antenna Systems and Technologies, ESA WPP-247, May 2005.

6. J. Zackrisson, "Wide Coverage Antennas", 21st Annual AIAA/USU Conference on Small Satellites, August 2007.

7. J. Zackrisson, "Wide Coverage Antenna Developments", TTC 2007 Workshop, ESA/ESOC, September 2007.

8. P. Ingvarson, M. Bonnedal, J. Wettergren, B. Wästberg, "A GPS Antenna for Precise Orbit Determination of The SWARM Satellites", EuCAP 2007, November 2007.

9. J Wettergren, M Bonnedal, P Ingvarson, B Wästberg, "Antenna for precise orbit determination", 59th IAC 2008.

10. M Öhgren, M Bonnedal, P Ingvarson, "Small and Lightweight GNSS Antenna for Precise Orbit Determination", 32nd ESA Antenna Workshop on Antennas for Space Applications, October 2010

11. M Öhgren, M Bonnedal, P Ingvarson, "GNSS Antenna for Precise Orbit Determination Including S/C Interference Predictions", EuCAP 2011, April 2011.